

Gene Expression Profile as a Precursor of Inflammation in Mouse Models: BFMI860 and C57BL/6NCrI

Ayca Dogan¹, Gudrun A. Brockmann²

¹Department of Physiology, Faculty of Medicine, Altinbas University, Istanbul, Turkiye

²Animal Breeding Biology and Molecular Genetics, Albrecht Daniel Thaer-Institute for Agricultural and Horticultural Sciences, Humboldt University of Berlin, Berlin, Germany

ORCID ID: A.D. 0000-0002-6020-8327; G.A.B. 0000-0002-4387-2947

Cite this article as: Dogan A, Brockmann GA. Gene expression profile as a precursor of inflammation in mouse models: BFMI860 and C57BL/6NCrI. *Experimed* 2024; 14(2): 73-84.

ABSTRACT

Objective: We aimed to investigate the differences in the immune response to body fat content between the genetically mutant obese BFMI860 (BFMI) mouse strain and the lean C57BL/6NcrI (B6) mouse strain as a control and the effects of obesity on gene expression on inflammation-related pathways in epididymal adipose tissue.

Materials and Methods: Six males from each strain were maintained on a standard maintenance diet (SMD) or a high-fat diet (HFD). At the age of 10 weeks, serum and epididymal adipose tissue samples were collected for cytokine and gene expression analyses. RNA samples from epididymal adipose tissue were hybridized using the microarray technique to study the quantitative transcript amounts of genes.

Results: Pathway analysis of gene expression data revealed no considerable development of inflammatory state in BFMI and B6 on SMD. Both strains responded to HFD distinctly; the inflammatory state was more prominent in the obese BFMI group than in the lean B6 group. Several genes, such as *Adipoq*, *NFkbia*, *Plaur*, *F2r*, *C3ar1*, and *Nfatc4* in pathways involved in the immune system have been found to be differentially regulated in BFMI mice. Under the condition of obesity in BFMI mice, the induction of inflammation-related pathways indicates an increased risk of insulin resistance, atherosclerosis, and cardiovascular disease.

Conclusion: This study identified distinct expression patterns of genes involved in inflammatory pathways, particularly those associated with the adipocytokine signaling pathway and complement and coagulation cascades, in the epididymal adipose tissue of BFMI and B6 mice. The BFMI strain is a valuable and promising model for clarifying the mechanisms underlying obesity and the activation of inflammation in adipose tissue.

Keywords: Obesity, high-fat diet, adipocytokine signaling pathway, complement and coagulation cascade

INTRODUCTION

The comorbidities associated with obesity are due to the infiltration and accumulation of pro-inflammatory macrophages in the adipose tissue, which trigger changes in the immune system through the production of inflammatory cytokines. Positive correlations between inflammatory cytokines such as tumor necrosis factor- α (TNF- α), monocyte chemoattractant protein 1 (MCP1), interleukin-6 (IL-6), and interleukin-8 (IL-8), and the degree

of adiposity in obese individuals have been presented through several studies (1). Increased circulating levels of inflammatory markers are associated with obesity-related pathologies. The distribution of adipose tissue affects these associations. Visceral adipose tissue is a major risk factor for insulin resistance, type 2 diabetes, cardiovascular disease, and metabolic syndrome (1). Therefore, visceral fat is considered as the most dangerous adipose tissue (2). It is known that obesity causes alterations in the transcript levels of genes in some pathways linking fat tissue metabolism to

Corresponding Author: Ayca Dogan **E-mail:** ayca.mollaoglu@altinbas.edu.tr

Submitted: 01.11.2023 **Revision Requested:** 03.03.2024 **Last Revision Received:** 22.06.2024 **Accepted:** 05.08.2024



Content of this journal is licensed under a Creative Commons Attribution-NonCommercial 4.0 International License.

the immune system (2). Therefore, to investigate the effects of obesity on the immune response, we examined the transcript levels of cytokines and pro-inflammatory genes involved in inflammation-related pathways including adipocytokine signaling pathway and complement and coagulation cascades, in the Berlin Fat Mouse Inbred 860 (BFMI) strain and the C57BL/6NcrJ (B6) strain. BFMI is genetically predisposed to obesity and characterized by high body fat mass, impaired fat oxidation (3), dysregulated cytokine production, and insulin resistance (4). The B6 strain is a lean inbred strain often used as a reference.

The objectives of the present study were, first, to detect differences in the immune response to body fat content between BFMI and B6 mice at the genetic level (strain effect) and, second, to investigate the effects of obesity on gene expression levels in inflammation-related pathways within each strain.

MATERIALS AND METHODS

Animals and Ethical Approval

BFMI and B6 (Charles River Laboratories, Sulzfeld, Germany) male mice were bred, fed, and grown until 10 weeks old in an animal facility at Humboldt University of Berlin, as described previously (3). In brief, we generated the BFMI860 strain from an outbred population. Founder mice were originally purchased from pet shops in Berlin and subsequently selected for low protein content, low body mass and high fat content, followed by high fatness for 58 generations before inbreeding. C57BL/6NcrJ mice (Charles River Laboratories, Sulzfeld, Germany) were used as controls. All experiments were

performed in accordance with the approval of the German Animal Welfare Authorities (approval no. G0152/04 and V54-19c20/15c MR 17/1).

Animal Feeding

BFMI (n=6) and B6 (n=6) mice were fed either with a standard maintaining diet (SMD) or high-fat diet (HFD), for 7 weeks. Following weaning at 3 weeks old, 6 male B6 mice were fed with SMD (V1534-000 ssniff R/M-H, ssniff Spezialdiäten GmbH, Soest, Germany) containing 12.8 MJ/kg metabolizable energy (9% of its energy from fat, 33% from protein content and 58% from carbohydrates). Additionally, 6 male BFMI mice were given an HFD (S8074-E010 ssniff EF R/M, ssniff Spezialdiäten GmbH, Soest, Germany) containing 19.1 MJ/kg metabolizable energy, with 45% of its energy from fat, 24% from protein, and 31% from carbohydrates. The SMD included soy oil as its source of fat, whereas the HFD included coconut oil and suet as its source of fat. The mice had *ad libitum* access to food and water. They were maintained at room temperature (22°C - 24°C) with a 12-hour light/dark cycle. The detailed composition and energy content of both diets were extensively documented by Wagener et al. (3). Mice were weighed weekly from the age of 3 weeks.

Intraperitoneal Glucose Tolerance Test (IPGTT)

After 12-14 h of fasting, we collected a baseline blood sample (fasting glucose at time zero) from 10-week-old mice. Each animal was given a single intraperitoneal injection of glucose (B. Braun, Melsungen, Germany) at a dose of 2 g/kg body weight. Blood was drawn from the tail tip 15, 30, 60, and 120 min after intraperitoneal glucose injection. Glucose concentrations

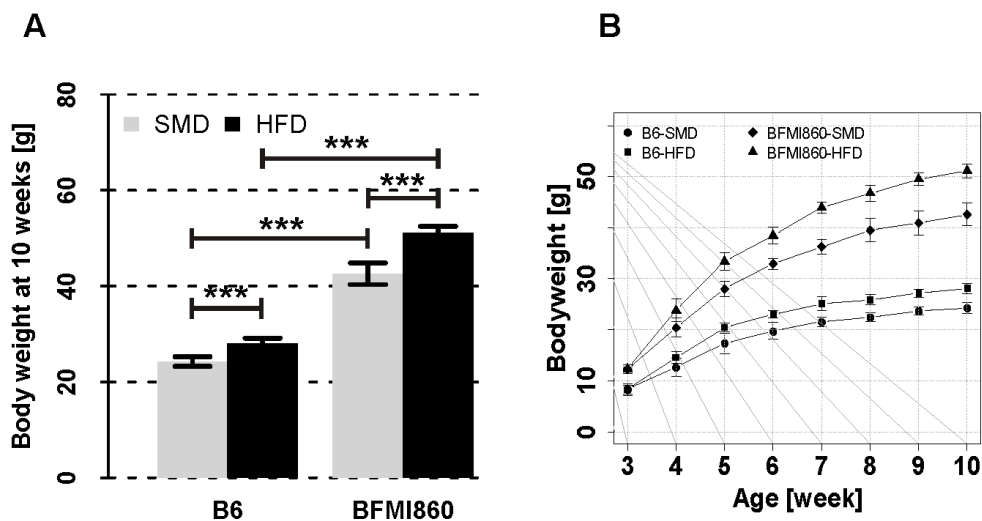


Figure 1A. Body weight at 10 weeks of age, **B.** Body weight development of BFMI and B6 males under either SMD or HFD from 3 to 10 weeks of age. Each point represents the mean weight and standard deviation (SD). Statistically significance difference; *, $p < 0.05$, **, $p < 0.01$, ***, $p < 0.001$.

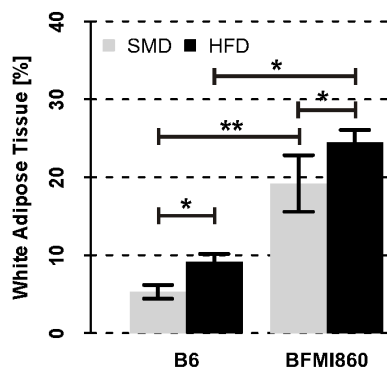


Figure 2. Percentage of white adipose tissue (WAT) to body weight of BFMI and B6 males under either SMD or HFD at 10 weeks of age. Values are mean \pm SD. Statistically significance difference; *: $p < 0.05$, **: $p < 0.01$, ***: $p < 0.001$.

were measured using an Ascensia Elite glucose analyzer (Bayer HealthCare, Leverkusen, Germany). For the determination of insulin levels, blood samples were drawn from the tail and extracted at 0, 30, 60, and 120 min after intraperitoneal injection of glucose and were determined by enzyme-linked immunosorbent assay (ELISA) as described.

Animal Euthanasia and Sample Collection

Ten-week-old male mice were anesthetized with isoflurane and decapitated after 2 hours of fasting period. Blood was collected at necropsy after cervical dislocation. Serum was recovered by centrifugation for 15 min at 600 g and used for cytokine measurements, and epididymal adipose tissue was used for gene expression analyses. Tissues were collected in liquid nitrogen and stored at -80°C until RNA preparation.

Measurement of Serum Parameters

Serum leptin, adiponectin, and insulin levels were measured by ELISA as described by Hantschel et al. (4). Leptin levels

Table 1. Differentially expressed genes in the adipocytokine signaling pathway in the epididymal adipose tissue.

MGI ID	Symbol	Gene name	BFMI vs B6 SMD			BFMI vs B6 HFD		
			Fold	FDR	p-value	Fold	FDR	p-value
99484	<i>Chuk</i>	conserved helix-loop-helix ubiquitous kinase	0.821	0.258	NS	0.739	0.002	<0.001
104741	<i>Nfkb1a</i>	nuclear factor of kappa light chain gene enhancer in B-cells inhibitor, alpha	0.947	NS	NS	4.094	0.000	<0.001
1342774	<i>Ppargc1a</i>	peroxisome proliferative activated receptor, gamma, coactivator 1 alpha	0.707	0.004	<0.001	0.735	0.036	NS
97374	<i>Npy</i>	neuropeptide Y	1.678	0.007	<0.001	1.592	0.000	<0.001
104740	<i>Ppara</i>	peroxisome proliferators activated receptor alpha	0.868	0.094	NS	0.737	0.000	<0.001
98214	<i>Rxra</i>	retinoid X receptor alpha	0.689	0.001	<0.001	0.614	0.000	<0.001
106675	<i>Adipoq</i>	adiponectin, C1Q and collagen domain containing	0.706	0.263	NS	0.458	0.001	<0.001
93830	<i>Adipor2</i>	adiponectin receptor 2	0.640	0.013	<0.001	0.593	0.040	NS
95755	<i>Slc2a1</i>	solute carrier family 2 (facilitated glucose transporter), member 1	1.105	NS	NS	2.108	0.023	<0.001
1201791	<i>Socs3</i>	suppressor of cytokine signaling 3	1.173	NS	NS	1.841	0.000	<0.001
98216	<i>Rxrg</i>	retinoid X receptor gamma	0.837	0.114	NS	0.595	0.000	<0.001

MGI, Mouse Genome Informatics; FDR, false discovery rates; SMD, standard maintenance diet; HFD, high-fat diet; BFMI, BFMI860 mouse strain; B6, C57BL/6NcrJ mouse strain; NS: not significant

The table shows all genes that were significantly differentially expressed at $p < 0.001$ and $\text{FDR} < 0.5$ in at least one of the comparisons between BFMI and B6 on SMD or BFMI and B6 on HFD. MGI ID refers to the gene identity number in Mouse Genome Informatics database (www.informatics.jax.org/genes.shtml).

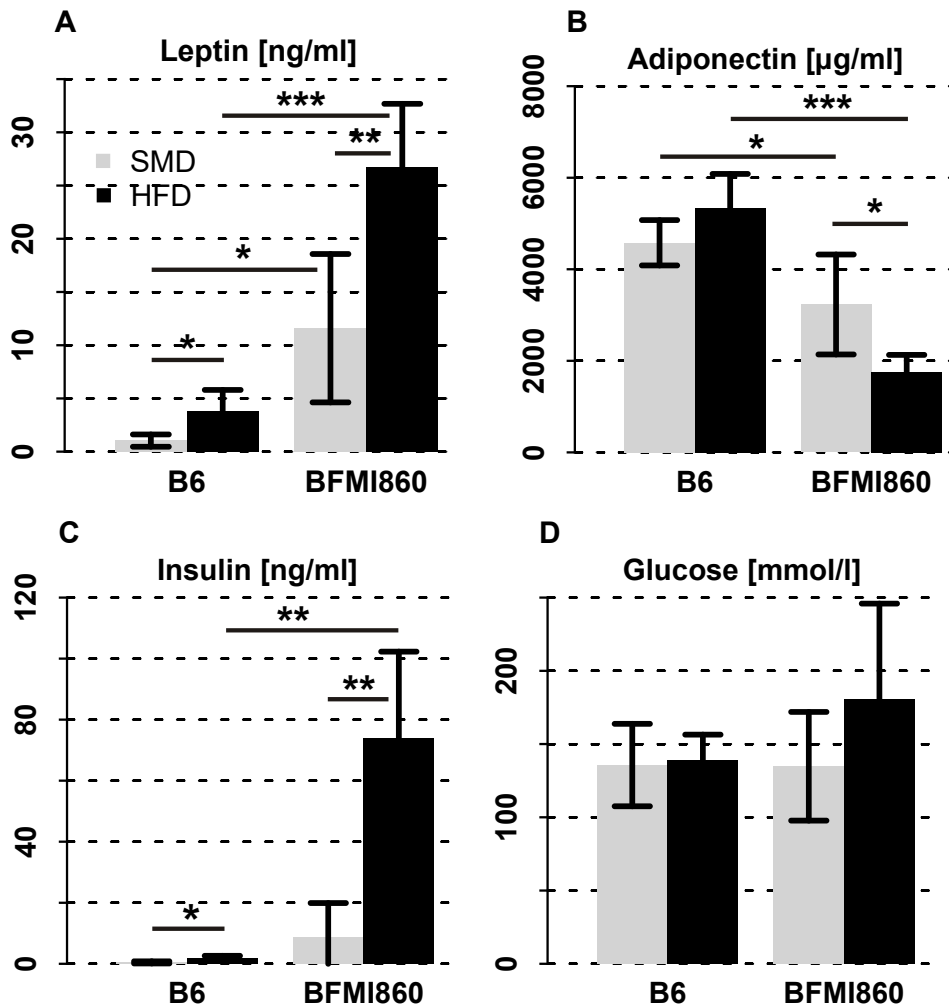


Figure 3. Serum levels of **A.** leptin, **B.** adiponectin, **C.** insulin, **D.** glucose at 10 weeks of age. Data are expressed as mean ± SD (n= 6). Statistically significance difference; *: p < 0.05, **: p < 0.01, ***: p < 0.001.

were determined using an m/rLeptin ELISA kit (Mediagnost, Reutlingen, Germany). Adiponectin levels were determined using a DuoSet ELISA Development kit (R&D Systems, Wiesbaden, Germany). Insulin levels were measured using a commercial Insulin Mouse Ultrasensitive ELISA (DRG Instruments GmbH, Marburg, Germany).

Gene Expression Analysis

Gene expression was measured using RNA isolated from epididymal adipose tissue of BFM1 and B6 mice at 10 weeks. RNA was extracted and gene expression was performed as described in Wagener et al. (3). The RNA samples of six animals of the four biological groups (B6-SMD / B6-HFD / BFM1-SMD / BFM1-HFD) were hybridized on Illumina Mouse WG-6 v1.1 Expression BeadChips using an Illumina BeadStation 500X.

The lists of differentially expressed genes in epididymal adipose tissue are illustrated in Table 1 for adipocytokine signaling pathway, and in Table 2 for the complement and coagulation cascades. Diet effects on the adipocytokine signaling pathway

and complement and coagulation cascades are shown in Tables 3 and 4, respectively. Differentially expressed genes in epididymal adipose tissue, in the interaction between strain and diet, and immune response-related pathways are noted in Tables 5 and 6.

Statistical Analyses

Fluorescence images of the Illumina Bead Arrays were translated into relative expression levels using the Bioconductor (5) package bead array (6) with standard parameter settings. The intensity values of the arrays were log2-transformed and quantile-normalized for fat tissue. The statistical analysis was performed using the R statistical software package (7). Differences in gene expression between BFM1 and B6 mice fed with either a SMD or a HFD and between HFD and SMD in either BFM1 or B6 mice were evaluated using two separate Student's t-test. To address multiple testing, false discovery rates (FDR) were calculated using a customized algorithm that was implemented in R. Where necessary, medians of fold-

Table 2. Differentially expressed genes in complement and coagulation cascade signaling pathway in the epididymal adipose tissue.

MGI ID	Symbol	Gene name	BFMI vs B6 SMD			BFMI vs B6 HFD		
			Fold	FDR	p-value	Fold	FDR	p-value
97611	<i>Plau</i>	plasminogen activator, urokinase	1.822	0.009	<0.001	2.101	0.004	<0.001
97612	<i>Plaur</i>	plasminogen activator, urokinase receptor	1.613	0.048	NS	1.965	0.010	<0.001
101802	<i>F2r</i>	coagulation factor II (thrombin) receptor	1.583	0.039	NS	2.438	0.001	<0.001
88381	<i>F3</i>	coagulation factor III	0.473	0.012	<0.001	1.354	0.131	NS
109325	<i>F7</i>	coagulation factor VII	2.971	0.001	<0.001	1.994	0.000	<0.001
103107	<i>F10</i>	coagulation factor X	2.404	0.020	<0.001	2.380	0.000	<0.001
105975	<i>H2-Bf</i>	histocompatibility 2 complement component	1.319	0.052	NS	2.576	0.006	<0.001
87931	<i>Adn</i>	complement factor D (adipsin)	0.320	0.014	<0.001	0.055	0.000	<0.001
88226	<i>C2</i>	complement component 2	0.201	0.000	<0.001	0.290	0.000	<0.001
105937	<i>Cfi</i>	complement component factor i	1.266	0.019	<0.001	1.577	0.002	<0.001
1097680	<i>C3ar1</i>	complement component 3a receptor 1	2.463	0.011	<0.001	4.237	0.000	<0.001

MGI ID, Mouse Genome Informatics ; FDR, false discovery rates; SMD, standard maintenance diet; HFD, high-fat diet; BFMI, BFMI860 mouse strain; B6, C57BL/6NcrI mouse strain; NS, not significant.

The table shows all genes that were significantly differentially expressed at p<0.001 and FDR<0.5 in at least one of the comparisons between BFMI and B6 on SMD or BFMI and B6 on HFD. MGI ID refers to the gene identity number in Mouse Genome Informatics database (www.informatics.jax.org/genes.shtml).

Table 3. Differentially expressed genes in the adipocytokine signaling pathway in the epididymal adipose tissue.

MGI ID	Symbol	Gene name	B6 HFD vs SMD			BFMI HFD vs SMD		
			Fold	FDR	p-value	Fold	FDR	p-value
107899	<i>Cd36</i>	Cd36 antigen	0.5	0.002	<0.001	1.2	0.874	NS
104741	<i>Nfkbia</i>	nuclear factor of kappa light chain gene enhancer in B-cells inhibitor, alpha	0.4	0.000	<0.001	1.6	0.297	NS
106675	<i>Adipoq</i>	adiponectin, C1Q and collagen domain containing	0.8	0.028	<0.001	0.5	0.131	NS

MGI, Mouse Genome Informatics; FDR, false discovery rates; SMD, standard maintenance diet; HFD, high-fat diet; BFMI, BFMI860 mouse strain; B6, C57BL/6NcrI mouse strain; NS, not significant.

The table shows all genes that were significantly differentially expressed at p<0.001 and FDR<0.5 in at least one of the comparisons between BFMI and B6 on SMD or BFMI and B6 on HFD. MGI ID refers to the gene identity number in the Mouse Genome Informatics (MGI) database (www.informatics.jax.org/genes.shtml).

Table 4. Differentially expressed genes in complement and coagulation cascade signaling pathway in the epididymal adipose tissue.

MGI ID	Symbol	Gene name	B6 HFD vs SMD			BFMI HFD vs SMD		
			Fold	FDR	p-value	Fold	FDR	p-value
88381	<i>F3</i>	coagulation factor III	0.5	0.020	<0.001	1.3	0.205	NS
98736	<i>Thbd</i>	thrombomodulin	0.4	0.011	<0.001	0.6	0.366	NS
105975	<i>H2-Bf</i>	histocompatibility 2 complement component	0.5	0.036	<0.001	0.9	0.658	NS
87931	<i>Adn</i>	complement factor D (adipsin)	1.0	0.779	NS	0.2	0.035	<0.001

MGI, Mouse Genome Informatics ; FDR, false discovery rates; SMD, standard maintenance diet; HFD, high-fat diet; BFMI, BFMI860 mouse strain; B6, C57BL/6Ncr1 mouse strain; NS, not significant.

The table shows all genes that were significantly differentially expressed at p<0.001 and FDR<0.5 in at least one of the comparisons between BFMI and B6 on SMD or BFMI and B6 on HFD. MGI ID refers to the gene identity number in Mouse Genome Informatics (MGI) database (www.informatics.jax.org/genes.shtml).

Table 5. Differentially expressed genes show interaction between strain and diet in the epididymal adipose tissue.

KEGG Pathway	MGI ID	Symbol	Gene Name	Fold
Adipocytokine signaling pathway	1194882	<i>Irs3</i>	insulin receptor substrate 3	0.4
	107899	<i>Cd36</i>	CD36 antigen	2.5
	98216	<i>Rxrg</i>	retinoid X receptor gamma	0.7
Adipocytokine signaling, T cell signaling, B cell signaling, and Toll-like receptor signaling pathway	1099800	<i>Nfkb2</i>	nuclear factor of kappa light polypeptide gene enhancer in B-cells	1.6
	104741	<i>Nfkb1a</i>	nuclear factor of kappa light chain gene enhancer in B-cells inhibitor, alpha	4.3
T cell signaling	88332	<i>Cd3e</i>	CD3 antigen, epsilon polypeptide	1.6
T cell signaling, Natural killer cell signaling	1920431	<i>Nfatc4</i>	nuclear factor of activated T-cells, cytoplasmic, calcineurin-dependent 4	1.9
T cell signaling, Natural killer cell signaling, Fc epsilon RI signalling pathway	1342293	<i>Lat</i>	linker for activation of T cells	2.3
B cell signaling	1096398	<i>Cd81</i>	CD81 antigen	1.4
Natural killer cell signaling	95904	<i>H2-K1</i>	histocompatibility 2, K1, K region	3.5
	1346866	<i>Map2k1</i>	mitogen activated protein kinase 1	2.5
Complement and coagulation cascades	88381	<i>F3</i>	coagulation factor III	2.9
	87931	<i>Adn</i>	complement factor D (adipsin)	0.2

KEGG, Kyoto Encyclopedia of Genes and Genomes; MGI, Mouse Genome Informatics.

The table shows all genes that were significantly differentially expressed at p<0.001 and FDR<0.5 in at least one of the comparisons between BFMI and B6 on SMD or BFMI and B6 on HFD. MGI ID refers to the gene identity number in the Mouse Genome Informatics (MGI) database (www.informatics.jax.org/genes.shtml).

Table 6. Gene annotations of differentially expressed genes in the epididymal adipose tissue.

BFMI vs B6 on HFD fat	Number of genes	Genes
Immune system		
Toll-like receptor signaling pathway	18	<u>Cxcl9</u> , <u>Irf5</u> , <u>Ly96</u> , <u>Ifna5</u> , <u>Fos</u> , <u>Tlr5</u> , <u>Tlr2</u> , <u>Spp1</u> , <u>Cd14</u> , <u>Tlr1</u> , <u>Tlr7</u> , <u>Myd88</u> , <u>Ccl4</u> , <u>Ccl3</u> , <u>Ticam2</u> , <u>Pik3cg</u> , <u>Nfkbia</u> , <u>Map2k1</u>
Leukocyte transendothelial migration	8	<u>Atp1b3</u> , <u>Rap1b</u> , <u>Vav1</u> , <u>Bcar1</u> , <u>Plcg2</u> , <u>Ncf2</u> , <u>Pik3cg</u> , <u>My19</u>
B cell receptor signaling pathway	14	<u>Cd72</u> , <u>Ptpn6</u> , <u>Sykb</u> , <u>Prkcb</u> , <u>Card11</u> , <u>Blnk</u> , <u>Kras</u> , <u>Fos</u> , <u>Vav1</u> , <u>Lilrb3</u> , <u>Btk</u> , <u>Plcg2</u> , <u>Pik3cg</u> , <u>Nfkbia</u>
Natural killer cell mediated cytotoxicity	19	<u>H2-K1</u> , <u>Cd48</u> , <u>Itgb2</u> , <u>Ptpn6</u> , <u>Fcgr4</u> , <u>Kras</u> , <u>Vav1</u> , <u>Plcg2</u> , <u>Grb2</u> , <u>Pik3cg</u> , <u>Sykb</u> , <u>Prkcb</u> , <u>Sh3bp2</u> , <u>Fcgr3</u> , <u>Ifna5</u> , <u>Tyrobp</u> , <u>Fcer1g</u> , <u>Lat</u> , <u>Map2k1</u>
Signaling molecules and interaction		
Cytokine-cytokine receptor interaction	27	<u>Vegfa</u> , <u>Ccl6</u> , <u>Cxcl9</u> , <u>Ccl24</u> , <u>Tnfsf13</u> , <u>Ccr5</u> , <u>Ccl2</u> , <u>Ccl4</u> , <u>Figf</u> , <u>Ccl3</u> , <u>Pf4</u> , <u>Il10</u> , <u>Ccl27a</u> , <u>Ccl17</u> , <u>Tspan7</u> , <u>Cxcl1</u> , <u>Ltbr</u> , <u>Ifna5</u> , <u>Tnfrsf17</u> , <u>Cxcl14</u> , <u>Ccl7</u> , <u>Cx3cr1</u> , <u>Pdk3</u> , <u>Ctf1</u> , <u>Il10rb</u> , <u>Ccl8</u> , <u>Bmp2</u>
BFMI vs B6 on SMD		
Immune system		
Leukocyte transendothelial migration	17	<u>Rock2</u> , <u>Cldn1</u> , <u>Ncf4</u> , <u>Esam</u> , <u>Actn1</u> , <u>Ctnna1</u> , <u>Ncf1</u> , <u>Gnai2</u> , <u>Cyba</u> , <u>Rapgef3</u> , <u>F11r</u> , <u>Cldn5</u> , <u>Gnai1</u> , <u>Mmp2</u> , <u>Mmp9</u> , <u>Rac2</u> , <u>Cxcr4</u>
Antigen processing and presentation	5	<u>Ctss</u> , <u>H2-Ea</u> , <u>Ifi30</u> , <u>Ctsb</u> , <u>Cd74</u>
Signaling molecules and interaction		
ECM-receptor interaction	11	<u>Col1a2</u> , <u>Col6a1</u> , <u>Itga6</u> , <u>Col6a2</u> , <u>Col1a1</u> , <u>Col3a1</u> , <u>Itga5</u> , <u>Vtn</u> , <u>Col4a1</u> , <u>Spp1</u> , <u>Lamb3</u>
Signal transduction		
Wnt signaling pathway	16	<u>Smad2</u> , <u>Rock2</u> , <u>Lrp6</u> , <u>Prkcb</u> , <u>Sfrp2</u> , <u>Rac3</u> , <u>Wnt2b</u> , <u>Wif1</u> , <u>Sfrp4</u> , <u>Smad4</u> , <u>Wnt2</u> , <u>Cxhc4</u> , <u>Sox17</u> , <u>Siah1a</u> , <u>Rac2</u> , <u>Fzd6</u>
HFD vs SMD in BFMI		
PPAR signaling pathway	5	<u>Scd1</u> , <u>Fabp3</u> , <u>Hmgcs2</u> , <u>Scd2</u> , <u>Ucp1</u>

MGI, Mouse Genome Informatics ; FDR, false discovery rates; SMD, standard maintenance diet; HFD, high-fat diet; BFMI, BFMI860 mouse strain; B6, C57BL/6Ncr1 mouse strain.
Down-regulated genes are underlined. Only annotations with corrected p ≤ 0.001 are shown. MGI ID refers to the gene identity number in the Mouse Genome Informatics (MGI) database (www.informatics.jax.org/genes.shtml).

changes, medians of significance values and FDR were used to define unique values for each gene, if multiple oligos existed and were measuring the expression of the same gene.

To measure the significance of the interaction between strain and diet, a 2 by 2 analysis of variance (ANOVA) was performed with the factors strain and diet for each probe within fat tissue:

$$\log_2(\text{expression}) = \mu + \text{strain} + \text{diet} + \text{strain: diet} + \epsilon$$

where μ is the probe mean, strain is either BFMI860 or B6, diet is either SMD or HFD, strain: diet is the interaction term and ϵ is the residual variance. The R/Bioconductor package *maanova*

(8) was used with the *maanova* functions, *read.madata*, *fitmaanova*, and *matest*.

Differentially expressed genes with p values <0.001 and FDRs <0.5 were considered statistically significant in ANOVA and Student's t-test.

Genes showing significant differences between groups were assigned to inflammatory-related pathways based on the Kyoto Encyclopedia of Genes and Genomes (KEGG) database (<http://www.genome.jp/kegg/>). Pathways were visualized using the software GenMAPP (9).

RESULTS

Weight Gain and Serum Parameters

At 10 weeks, BFMI males were nearly two times as heavy as B6 males (Figure 1A). BFMI mice were already heavier at the early age of 3 weeks (Figure 1B). Body weight gain was markedly higher in the HFD group than in the SMD group in both strains. In addition, BFMI mice stored proportionally more fat than B6 in response to HFD (Figure 2).

Serum concentrations of leptin, adiponectin, insulin, and glucose were compared between BFMI and B6 control mice fed SMD and HFD. As expected, serum leptin levels were higher in BFMI mice than in B6 mice on both diets due to the higher body fat mass in BFMI (Figure 3A). Serum adiponectin levels were increased in B6 mice and decreased in BFMI mice on HFD (Figure 3B). Therefore, the changes in adiponectin levels in response to different diets were strain-dependent. BFMI mice on HFD exhibited high blood glucose levels. No significant change in blood glucose levels was observed in B6 mice (Figure 3D). In addition, serum insulin levels were markedly increased in response to HFD in BFMI mice but not in B6 mice (Figure 3C).

Gene Expression Analysis

We initially investigated the adipocytokine signaling pathway to identify differences in the regulation of gene expression that cause subsequent metabolic system alterations. Then, we examined the complement and coagulation cascades that were significantly altered in epididymal fat tissue. Subsequently, we studied the B-cell receptor, T-cell receptor, toll-like receptor, and natural killer cell signaling pathways to explore the interaction between strain and diet in epididymal fat tissue. Genes were considered differentially expressed if $p < 0.001$ and $FDR < 0.5$ within affected pathways.

The differentially expressed genes in epididymal adipose tissue belonging to different pathways are presented in Tables 1 and 2.

Strain Effect

Adipocytokine Signaling Pathway

KEGG analysis revealed that the adipocytokine signaling pathway was differentially expressed between BFMI and B6 mice. Two and seven of the 67 genes in this pathway were differentially expressed between these strains on SMD and HFD, respectively (Table 1). The expressions of *Ppargc1a* and *Adipor2* were significantly down-regulated in BFMI vs. B6 mice fed with SMD. In the case of HFD, we detected decreased *Adipoq*, *Chuk*, *Ppara*, and *Rxrg* expressions and markedly increased *Nfkb1a*, *Socs3*, and *Slc2a1* expressions in BFMI vs. B6 mice. We also observed higher leptin and lower *Irs1* transcript levels in the BFMI group, although these alterations were not statistically significant.

Complement and Coagulation Cascades

Group analysis of the differential gene expression pattern provided evidence that the complement and coagulation cascades were up-regulated in BFMI vs. B6 mice. Five out of 63 genes were up-regulated, while three were down-regulated in BFMI vs. B6 mice on SMD; eight genes were up-regulated and two were down-regulated on HFD, respectively. Among these genes, transcript levels of *H2-Bf* increased and *F3* decreased dissimilarly in BFMI vs. B6 mice on HFD and SMD, respectively. On HFD, *Plaur* and *F2r* were up-regulated (Table 2). We detected increased transcript levels in *Plaur*, *F7*, *F10*, *Cfi*, and *C3ar1* and decreased expression in *Adn* and *C2* of BFMI vs. B6 in both feeding groups.

Diet Effect

Adipocytokine Signaling Pathway

We found that expression of *Irs3*, *Cd36*, *Nfkb1a*, and *Adipoq* was significantly reduced in HFD vs SMD in B6 mice (Table 3). However, no marked alterations were determined in the gene expression of BFMI mice.

Complement and Coagulation Cascades

Decreased expressions of *F3*, *thrombomodulin* (*Thbd*), and *H2-Bf* genes were observed in B6 mice in HFD vs. SMD (Table 4). We detected decreased *Adn* expression, which was only differentially expressed in BFMI mice.

Effect of Interaction Between Strain and Diet

KEGG analysis identified T-cell receptor and natural killer cell signaling pathways that were significantly up-regulated in the epididymal adipose tissue with respect to strain and diet. The genes *Nfatc4* and *Lat*, which contribute to both pathways, were differentially expressed. In the T-cell, B-cell, and toll-like receptor signaling pathways, *Nfkb2* and *Nfkb1a* were differentially expressed. The expressions of all four genes were significantly increased in (BFMI on HFD vs. SMD) vs. (B6 on HFD vs. SMD), indicating the effects of interaction between strain and diet. We also detected decreased *Irs3* and increased *Cd36*, *Cd3e*, and *Cd81* expression in BFMI mice (Table 5).

Data Mining

To detect differentially expressed genes that did not belong to any of the analyzed pathways, genes were annotated using GeneCodis. The differentially expressed genes were then assigned to related pathways. Due to the large dataset size, several pathways that could affect the immune response were selected to provide an overview of inflammation. The most dramatically modulated genes, which are not involved in the discussed pathways, were observed in BFMI vs. B6 mice on HFD. The complete list of differentially expressed genes (up- and down-regulated) is shown in Table 6.

Analyzing the diet effects (HFD vs SMD), the genes in PPAR signaling pathways were differentially expressed in BFMI mice.

Among the regulated genes, the expression of ubiquitin D (Ubd) was 15-fold higher in HFD in contrast to SMD. The expressions of *cathepsin S (Ctss) b* and *Col1a2* were also up-regulated (20-fold and 11-fold, respectively) in BFMI on HFD mice compared to SMD mice (6-fold and 2-fold, respectively).

DISCUSSION

This study aimed to identify genetic variances in the immune response to body fat content between BFMI and B6 mice, as well as to assess the influence of obesity on gene expression in inflammation-related pathways. We found that the expression of several genes related to the immune system was dysregulated in the adipocytokine signaling pathway and complement and coagulation cascades in the epididymal adipose tissue of BFMI mice on the HFD diet.

Adipocytokine Signaling Pathway

The results indicated that the response to dietary fat is influenced by genetic background (strain effect). The expressions of *Adipoq*, *Chuk*, *Ppara*, *Rxrg*, *Nfkbia*, *Socs3*, and *Slc2a1* were dysregulated in BFMI mice on HFD. Several studies in humans and rodents have provided evidence of the anti-diabetic, anti-atherogenic, and anti-inflammatory activities of *Adipoq* (10). Therefore, lower transcript levels of the *Adipoq* gene in BFMI mice may reduce adiponectin sensitivity, which could finally abet insulin resistance in BFMI vs. B6 mice. Low adiponectin transcript levels in the epididymal adipose tissue might be a key link the activation of the immune system in adipose tissue of BFMI males. The markedly decreased *Adipoq* expression in epididymal adipose tissue corresponds well with reduced serum adiponectin concentrations in BFMI mice on HFD. In healthy individuals, adiponectin suppresses the activation of TNF- α -mediated nuclear factor kappa B (NF- κ B) (11). In addition, *Nfkbia* plays a role in the termination of NF- κ B activity by binding to it (12). In our study, the down-regulation of *Adipoq* was in line with the up-regulation of *Nfkbia* and denoted the suppression of NF- κ B activation.

Up-regulation of *Socs3*, a down-regulated target of NF- κ B, supported this finding. As an important transcription factor, NF- κ B regulates mediators of immune response, cell apoptosis, inflammation, embryonic development, and the cell cycle (11).

Socs3, which is also up-regulated in BFMI mice, suppresses cytokine signaling. *Socs3* is a negative regulator of the insulin signaling pathway. It suppresses insulin-stimulated glucose uptake by inhibiting *Irs1* in epididymal adipose tissue. This may lead to local insulin resistance (13). The higher leptin mRNA levels together with the up-regulated *Socs3* and reduced *Irs1* transcript levels in BFMI vs. B6 mice on HFD are in agreement with the study of Mori et al. (14), which showed that increased *Socs3* is a main regulator of diet-induced leptin and insulin resistance in Nestin-Cre and Synapsin1-Cre mice. Simultaneous

up-regulation of *Socs3* and down-regulation of *Adipoq* transcript levels in BFMI indicate impaired insulin sensing and activation of local inflammation in adipose tissue in response to the HFD.

The up-regulation of fat-cell-specific glucose transporter 1 (*Slc2a1*) provides evidence for higher glucose uptake in epididymal adipose tissue of BFMI vs. B6 mice, particularly on HFD. Despite suppressed insulin-stimulated glucose uptake due to increased *Socs3* expression, this finding is consistent with studies on type 2 diabetic animals, which have also shown a significant increase in basal glucose uptake into adipose tissue as insulin-stimulated glucose uptake was inhibited (15).

The results suggest that the genes *Adipoq*, *Nfkbia*, and *Socs3* in the adipocytokine signaling pathway are most likely to link obesity to adipose-specific inflammation.

The diet effect was particularly notable in B6 mice on HFD. In this strain, glucose and fatty acid transport may be decreased, as indicated by the down-regulation of *Irs3* and *Cd36* expression, respectively. Adiponectin, an anti-inflammatory cytokine, inhibits the activation of NF- κ B. Down-regulation of *Adipoq* together with *Irs3* and *CD36* expression may indicate the onset of inflammation in HFD-fed B6 mice. Gene expression was not influenced by diet in BFMI mice.

Complement and Coagulation Cascades

Our results showed that the genetic background (strain effect) significantly affected the alterations in gene expression caused by diet in the complement and coagulation cascades. The complement system bridges innate and acquired immunity and can be activated via three pathways: classical, lectin, and alternative (16). Genes of the classical and alternative pathways were activated in BFMI mice vs. B6. Among the factors of the complement cascade, the complement anaphylatoxins C3a and C5a play an important role in the metabolism of the entire body, energy balance, and the pathogenesis of diabetes and metabolic syndrome (17). They act as chemoattractants and trigger inflammation through their receptors C3ar1 and C5ar1 (16). These receptors have been identified as major positive regulators of insulin secretion, and their inhibitory effects on glucose-stimulated insulin secretion were demonstrated by Atanes et al. (17). Therefore, increased expression of *C3ar1* may imply that complement anaphylatoxins C3a and C5a activation could be in the early stage, and they may affect insulin secretion in BFMI vs. B6 mice on both SMD and HFD.

Complement Factor B (H2-Bf), which is also increased in BFMI mice, is an essential protein in the alternative pathway of complement activation. Moreno-Navarrete et al. (18) reported that increased expression of H2-Bf is associated with activation of the alternative complement pathway, which is linked to insulin resistance, obesity, and metabolic complications. The increased transcript levels of *H2-Bf* indicated that the alternative pathway, which promotes insulin resistance and atherosclerosis, was activated in the HFD group. Our results also

showed that the activity of the alternative pathway changed depending on the dietary effect.

The complement system interacts with the coagulation system (19). Tissue factor (TF, F3) is the main cellular initiator of the coagulation cascade and serves as a receptor for activated factor VII (FVIIa) and forms the TF-activated factor VII complex (20). The TF-activated factor VII complex mainly triggers coagulation as well as angiogenesis, inflammation, and atherosclerosis (20). Decreased *F3* expression level indicates that the coagulation cascade may not be activated in BFMI vs. B6 mice fed with SMD. The blood clotting factor F7 is important for the initiation of F3-induced extrinsic coagulation levels that are related to plasma triglyceride levels (21). The TF-activated factor VII complex activates protease-activated receptor 1 (F2r, PAR1), which contributes to adipogenesis and promotes inflammation and angiogenesis (22). Furthermore, a strong association was found between F2r and basal glucose levels in high-fat-fed mice (23). Plasminogen activator urokinase receptor (Plaur) contributes to macrophage infiltration in white adipose tissue (24). Therefore, increased transcript levels of Plaur and F2r may indicate macrophage migration and initiation of inflammation in the epididymal adipose tissue of BFMI mice on HFD.

The diet only significantly affected the expression of the *Adipsin (Adn)* gene in BFMI mice. Adn is an adipocyte serine protease that participates in triacylglycerol synthesis in human adipocytes, triggers insulin secretion, maintains β -cell function, and promotes adipocyte differentiation through C3a-C3aR signaling. Its expression is reduced in BFMI mice as well as in obese and diabetic animal models (25). In the current study, the up-regulated expression of *C3ar1* and down-regulated expression of *Adn* indicated that adipogenesis was underway in the animals and their energy balance was disturbed. Thbd is a cell surface-expressed glycoprotein that is involved in coagulation, fibrinolysis, complement activation, inflammation, and cell proliferation (26). Complement and coagulation cascades may not be activated as the expression of *F3*, *H2-Bf*, and *Thbd* is down-regulated in B6 mice. A recent study showed that dysregulated thrombin activity, including Thbd and fibrin, promotes obesity (27).

The differentially expressed genes *Nfatc4*, *Lat*, *Nfkb2* and *Nfkbia* in BFMI vs B6 on HFD vs. SMD indicate the effects of the interaction between strain and diet. Decreased *Irs3* and increased *Cd36*, *Cd3e*, and *Cd81* expressions were also detected in BFMI mice. In most cell types, NF- κ B is inactive in the cytoplasm, likely because of the inhibitory effect of *Nfkbia*. The activation of NF- κ B depends on the phosphorylation of *Nfkbia* by the inhibitor of κ B (I κ B) kinase (IKK). This modification leads to free NF- κ B that translocates to the nucleus. It regulates the transcription of response genes encoding chemokines, cytokines, adhesion molecules, inflammation-associated enzymes and inhibitors of apoptosis (12). It can therefore be suggested that the up-regulation of *Nfkbia* in BFMI mice may enhance the inflammatory response in epididymal adipose tissue. The Nfat group of transcription factors is an essential

component in cytokine gene expression upon T-cell activation. Kim et al. (28) reported that *Nfatc4* and *Atf3* negatively regulate adiponectin gene transcription. Thus, *Nfatc4* may contribute to decreased adiponectin expression. Yang et al. (29) demonstrated that *Nfatc4* contributes also to glucose and insulin metabolism. Increased *Nfatc4* expression in BFMI, together with reduced adiponectin concentration, may lead to increased insulin resistance. The linker for activation of T-cells (*Lat*) acts as a transmembrane scaffold protein critical for T-cell development and activation (30). Therefore, the up-regulation of *Lat* implies the activation of T-cells. Our results provide evidence that dysregulation of *Nfkbia* and *Nfatc4* in particular may affect the activation of the signaling cascade of obesity-induced inflammation.

Irs3 is important in Glut4 translocation and glucose transport in primary adipocytes (31). Reduced *Irs3* transcript levels indicate decreased glucose transport, as indicated by up-regulated *Socs3* expression in the adipocytokine signaling pathway. Increased fatty acid transport in HFD was supported by the up-regulation of *CD36*, which facilitates fatty acid uptake into muscle and adipose tissue (32). Oguri et al. (33) found that loss of *CD81* causes diet-induced weight gain, glucose intolerance, insulin resistance, and adipose tissue inflammation. Thus, *CD81* expression may be increased to prevent some metabolic disorders.

We also analyzed several pathways related to the immune response to provide a comprehensive assessment of inflammation. The genes exhibiting the most significant changes were identified in BFMI vs. B6 mice on HFD. Their gene expression profiles demonstrated that the number of significantly expressed genes associated with the immune system was higher in HFD than in SMD. In HFD, the regulated genes were detected only in the Toll-like receptor, B-cell receptor, and natural killer cell signaling pathways. These results indicate that these pathways may play a role in the differences between BFMI and B6 mice in terms of immune processes in adipose tissue.

The diet effect was significant only for the genes in the PPAR signaling pathways that showed differential expression in BFMI mice in HFD vs SMD.

The expression of *ubiquitin D (Ubd)* was up-regulated in BFMI on HFD compared with SMD. Ubd is involved in protein degradation and apoptosis (34) and mediates NF- κ B activation. It is not currently annotated in a pathway. The expression of *cathepsin S (Ctss) b* and *Col1a2* was up-regulated in BFMI on SMD mice. The change in *Ctss* expression is noteworthy in terms of their pathological effects. Previous studies have reported that it provides a molecular link between obesity and the development of cardiovascular disease (35). Moreover, Hsing et al. (36) noted that *Ctss* deficiency led to decreased diabetes incidence. These results were expected given that BFMI has 4 times more fat stored in SMD compared to B6 at 10 weeks of age.

The results of the present study revealed clear differences between the two strains. In general, we observed more differentially expressed genes in BFMI vs. B6 fed an HFD. It is evident that the effect of HFD on the aforementioned systems (immune, endocrine signaling molecules and interaction and signal transduction system) in adipose tissue is more profound in BFMI than in B6 mice. In particular, genes associated with immune system pathways were significantly up-regulated in the epididymal adipose tissue of BFMI mice. The immune response signal could be attributed to adipose tissue macrophages, which are involved in the immune system. It has already been shown that obesity causes inflammatory changes in the body (16).

CONCLUSIONS

Our results show that increased fat deposition in adipose tissue activates signaling cascades leading to increased inflammatory gene expression in both strains. BFMI mice are more responsive to HFD with obesity than B6 mice. This may be due to the different genetic compositions of these strains, as BFMI is already obese on SMD in contrast to B6. It is expected that most processes involved in the inflammatory response are significantly up-regulated in the epididymal adipose tissue of BFMI mice as a result of obesity. It is noteworthy that genes involved in the adipocytokine signaling pathway and the complement and coagulation cascades were differentially expressed between BFMI and B6 mice fed the same diet. Genes in immune-related pathways were also differentially regulated. These results imply that genotype plays an important role in obesity-induced inflammation. Inflammatory adipokines or proteins appear to function significantly in the “low-grade inflammatory state” in BFMI on SMD and more so on HFD, but also in B6 mice on HFD. When they enter the circulation, a cluster of metabolic abnormalities, such as insulin resistance and activation of complement cascades, can be induced and may be linked to an increased risk of diabetes and atherosclerosis. In addition, the interaction between strain and diet was very likely to have an impact on the inflammatory signaling network. The implication for humans is that genetic predisposition is not the only contributor to disease risk factors, but that genetic predisposition together with diet may activate a critical pathway leading to increased disease risk and further manipulation of obesity.

Acknowledgements

We thank Helge Gössling for microarray experiments, Ralf Bortfeldt for support in bioinformatics, Asja Wagener, Reinhard Schiefler, Katrin Beck, and Ulf Kiesling for mouse husbandry, and Pamela Kepper for technical assistance. This research was supported by grants from the German National Genome Research Network (NGFN: 01GS0486, 01GS0829), grants from the German Research Foundation (GRK1209) and the German Network for Systems Genetics (GeNeSys).

Ethics Committee Approval: All experiments were performed in accordance with the approval of the German Animal Welfare Authorities (approval no. G0152/04 and V54-19c20/15c MR 17/1).

Peer-review: Externally peer-reviewed.

Author Contributions: Conception/Design of Study- G.B.; Data Acquisition: A.D., G.B.; Data Analysis/Interpretation: A.D., G.B.; Drafting Manuscript- A.D.; Critical Revision of Manuscript- G.B.; Final Approval and Accountability- A.D., G.B.

Conflicts of Interests: The authors declare that they have no competing interests.

Financial Disclosure: This research was supported by grants from the German National Genome Research Network (NGFN: 01GS0486, 01GS0829), grants from the German Research Foundation (GRK1209) and the German Network for Systems Genetics (GeNeSys).

REFERENCES

1. Phillips CL, Grayson BE. The immune remodel: Weight loss-mediated inflammatory changes to obesity. *Exp Biol Med* (Maywood) 2020; 245(2): 109-121.
2. Mikhailova SV, Ivanoshchuk DE. Innate-Immunity Genes in Obesity. *J Pers Med* 2021; 11(11): 1201.
3. Wagener A, Goessling HF, Schmitt AO, Muel S, Gruber AD, Reinhardt R, et al. Genetic and diet effects on Ppar- α and Ppar- γ signaling pathways in the Berlin Fat Mouse Inbred line with genetic predisposition for obesity. *Lipids Health Dis* 2010; 9: 99.
4. Hantschel C, Wagener A, Neuschl C, Teupser D, Brockmann GA. Features of the metabolic syndrome in the Berlin Fat Mouse as a model for human obesity. *Obes Facts* 2011; 4(4): 270-7.
5. Reimers M, Carey VJ. Bioconductor: an open source framework for bioinformatics and computational biology. *Methods Enzymol* 2006; 411: 119-34.
6. Dunning MJ, Smith ML, Ritchie ME, Tavare S. beadarray: R classes and methods for Illumina bead-based data. *Bioinformatics* 2007; 23: 2183-4.
7. Ihaka R, Gentleman R. A language for data analysis and graphics. *J Comp Graph Statistics* 1996; 5: 299-314.
8. Cui X, Churchill GA. Statistical tests for differential expression in cDNA microarray experiments. *Genome Biol* 2003; 4: 210.
9. Dahlquist KD, Salomonis N, Vranizan K, Lawlor SC, Conklin BR. GenMAPP, a new tool for viewing and analyzing microarray data on biological pathways. *Nat Genet* 2002; 31: 19-20.
10. Von Frankenberg AD, Reis AF, Gerchman F. Relationships between adiponectin levels, the metabolic syndrome, and type 2 diabetes: A literature review. *Arch Endocrinol Metab* 2017; 61: 614-22.
11. Choi HM, Doss HM, Kim KS. Multifaceted physiological roles of adiponectin in inflammation and diseases. *Int J Mol Sci* 2020; 21(4): 1219.
12. Ghosh S, Karin M. Missing pieces in the NF-kappaB puzzle. *Cell* 2002; 109 Suppl: S81-96.
13. Wunderlich CM, Hövelmeyer N, Wunderlich FT. Mechanisms of chronic JAK-STAT3-SOCS3 signaling in obesity. *JAKSTAT* 2013; 2(2): e23878.
14. Mori H, Hanada R, Hanada T, Aki D, Mashima R, Nishinakamura H, et al. Socs3 deficiency in the brain elevates leptin sensitivity and confers resistance to diet-induced obesity. *Nat Med* 2004; 10: 739-43.
15. Talior I, Yarkoni M, Bashan N, Eldar-Finkelman H. Increased glucose uptake promotes oxidative stress and PKC-delta activation in adipocytes of obese, insulin-resistant mice. *Am J Physiol Endocrinol Metab* 2003; 285: E295-302.

16. Al Haj Ahmad RM, Al-Domi HA. Complement 3 serum levels as a pro-inflammatory biomarker for insulin resistance in obesity. *Diabetes Metab Syndr* 2017; 11 Suppl 1: S229-32.
17. Atanes P, Ruz-Maldonado I, Pingitore A, Hawkes R, Liu B, Zhao M, et al. C3aR and C5aR1 act as key regulators of human and mouse β -cell function. *Cell Mol Life Sci* 2018; 75(4): 715-26.
18. Moreno-Navarrete JM, Martínez-Barricarte R, Catalán V, Sabater M, Gómez-Ambrosi J, Ortega FJ, et al. Complement factor H is expressed in adipose tissue in association with insulin resistance. *Diabetes* 2010; 59(1): 200-9.
19. Shim K, Begum R, Yang C, Wang H. Complement activation in obesity, insulin resistance, and type 2 diabetes mellitus. *World J Diabetes* 2020;11(1):1-12.
20. Bernardi F, Mariani G. Biochemical, molecular and clinical aspects of coagulation factor VII and its role in hemostasis and thrombosis. *Haematologica* 2021; 106(2): 351-62.
21. Morrissey JH. Tissue factor interactions with factor VII: measurement and clinical significance of factor VIIa in plasma. *Blood Coagul Fibrinolysis* 1995; 6 Suppl 1: S14-19.
22. Yi X, Wu P, Liu J, Gong Y, Xu X, Li W. Identification of the potential key genes for adipogenesis from human mesenchymal stem cells by RNA-Seq. *J Cell Physiol* 2019; 234(11): 20217-27.
23. Macias-Velasco JF, St Pierre CL, Wayhart JP, Yin L, Spears L, Miranda MA, et al. Parent-of-origin effects propagate through networks to shape metabolic traits. *Elife* 2022; 11: e72989.
24. Canello R, Rouault C, Guilhem G, et al. Urokinase plasminogen activator receptor in adipose tissue macrophages of morbidly obese subjects. *Obes Facts* 2011; 4(1): 17-25.
25. Song NJ, Kim S, Jang BH, Chang SH, Yun UJ, Park KM, et al. Small molecule-induced complement factor D (Adipsin) promotes lipid accumulation and adipocyte differentiation. *PLoS One* 2016; 11(9): e0162228.
26. Van de Wouwer M, Plaisance S, De Vriese A, Waelkens E, Collen D, Persson J, et al. The lectin-like domain of thrombomodulin interferes with complement activation and protects against arthritis. *J Thromb Haemost* 2006; 4: 1813-24.
27. Kopec AK, Abrahams SR, Thornton S, Palumbo JS, Mullins ES, Divanovic S, et al. Thrombin promotes diet-induced obesity through fibrin-driven inflammation. *J Clin Invest* 2017; 127(8): 3152-66.
28. Kim HB, Kong M, Kim TM, Suh YH, Kim WH, Lim JH, et al. NFATc4 and ATF3 negatively regulate adiponectin gene expression in 3T3-L1 adipocytes. *Diabetes* 2006; 55: 1342-52.
29. Yang TTC, Suk HY, Yang XY, Olabisi O, Yu RYL, Durand J, et al. Role of transcription factor NFAT in glucose and insulin homeostasis. *Mol Cell Biol* 2006; 26: 7372-87.
30. Zhang W, Sloan-Lancaster J, Kitchen J, Tribble RP, Samelson LE. LAT: the ZAP-70 tyrosine kinase substrate that links T cell receptor to cellular activation. *Cell* 1998; 92: 83-92.
31. Zhou L, Chen H, Xu P, Cong LN, Sciacchitano S, Li Y, et al. Action of insulin receptor substrate-3 (IRS-3) and IRS-4 to stimulate translocation of GLUT4 in rat adipose cells. *Mol Endocrinol* 1999; 13: 505-14.
32. Son NH, Basu D, Samovski D, Pietka TA, Peche VS, Willecke F, et al. Endothelial cell CD36 optimizes tissue fatty acid uptake. *J Clin Invest* 2018; 128(10): 4329-42.
33. Oguri Y, Shinoda K, Kim H, Alba DL, Bolus WR, Wang Q, et al. CD81 controls beige fat progenitor cell growth and energy balance via FAK signaling. *Cell* 2020; 182(3): 563-77.e20.
34. Canaan A, Yu X, Booth CJ, Lian J, Lazar I, Gamfi SL, et al. FAT10/ diubiquitin-like protein-deficient mice exhibit minimal phenotypic differences. *Mol Cell Biol* 2006; 26: 5180-9.
35. Rodgers KJ, Watkins DJ, Miller AL, Chan PY, Karanam S, Brissette WH, et al. Destabilizing role of cathepsin S in murine atherosclerotic plaques. *Arterioscler Thromb Vasc Biol* 2006; 26: 851-6.
36. Hsing LC, Kirk EA, McMillen TS, Hsiao SH, Caldwell M, Houston B, et al. Roles for cathepsins S, L, and B in insulinitis and diabetes in the NOD mouse. *J Autoimmun* 2010; 34: 96-104.